Stress analysis of laminated glass with different interlayer materials

Alexandria Engineering Journal (2012) 51, 61–67

Alexandria University

Alexandria Engineering Journal

www.elsevier.com/locate/aej
www.sciencedirect.com

Stress analysis of laminated glass with different interlayer materials

Mostafa M. El-Shami [a,b,*], Scott Norville [b], Yasser E. Ibrahim [c]

[a] *Civil Engineering Department, Menoufia University, Egypt*
[b] *Civil and Environmental Engineering Department, Texas Tech. University, USA*
[c] *Construction Engineering Department, College of Engineering, Dammam University, Saudi Arabia*

Received 11 November 2010; accepted 1 April 2012
Available online 24 August 2012

KEYWORDS

Finite element;
Architectural glass;
Laminated glass;
Experimental

Abstract The use of window glass in building design is becoming increasingly popular. Laminated glass has gained popularity as a suitable and practical alternative to monolithic and insulating glass in many design situations. Laminated glass plate performance is influenced by several factors such as glass thickness, glass type, temperature, aspect ratio, load duration, and hardness of the interlayer material. A new higher order finite element model (presented by the first two authors) using 9-noded quadrilateral elements was applied to investigate laminated glass plates with both different interlayer materials. An experimental load-testing program is described. Two types of interlayer materials, regular polyvinyl butyral and strong formulation of polyvinyl butyral were used. First, simply supported rectangular laminated glass plates with regular polyvinyl butyral interlayer with aspect ratios 1–5 under different temperatures were tested. Second, one set of laminated glass plates with the strong formulation of polyvinyl butyral interlayer was tested under room temperature. The experimental and theoretical results are compared and discussed. In general, the performance of laminated glass with regular polyvinyl butyral interlayer is closer to that of layered glass at higher temperature. Also, laminated glass with strong formulation of polyvinyl butyral interlayer has a significantly larger load resistance than similar regular polyvinyl butyral samples.

1. Introduction

The use of window glass in building design is becoming increasingly popular. Laminated glass (LG) has gained popularity as a suitable and practical alternative to monolithic and insulating glass in many design situations. LG consists of two plates of glass joined by an elastomeric interlayer to form a unit. The most prevalent interlayer material used in architectural glazing is polyvinyl butyral; PVB, which comes off the production line as an opaque, flexible sheet that becomes clear during the lamination process. Another strong

* Corresponding author at: Civil and Environmental Engineering Department, Texas Tech University, Lubbock, TX 79409-1023, USA. E-mail address: mostafa.el-shami@ttu.edu (M.M. El-Shami).

Peer review under responsibility of Faculty of Engineering, Alexandria University.

Production and hosting by Elsevier

1110-0168 © 2012 Faculty of Engineering, Alexandria University. Production and hosting by Elsevier B.V. All rights reserved.
http://dx.doi.org/10.1016/j.aej.2012.07.008

formulation of polyvinyl butyral, called HG/MD has recently become more popular in LG as an interlayer material. There is a growing interest in understanding the effect of temperature on LG and its performance. The two most important factors affecting LG strength and behavior are load duration and temperature.

Considerable research has been done on laminated glass plates. Quenett [1] studied LG units subjected to both bending and impact loads. His research led to the conclusion that the behavior of LG is governed by the material properties of the interlayer and its thickness. Hooper [2] has shown that the bending of laminated glass beams is dependent on the thickness and shear modulus of the interlayer. Linden et al. [3] conducted non-destructive tests on monolithic layered and LG lite specimens instrumented with strain gauges. They found that LG lite strength and monolithic glass lite strength appeared to be equivalent at normal temperatures. Linden et al. [4] studied two different plate geometries with two interlayer thicknesses at room temperature and at 77 °C. They reported that LG lite is stronger than monolithic at room temperature and weaker at 77 °C for the same rectangular dimensions and nominal glass thickness. Nagalla et al. [5] advanced theoretical work comparing layered glass to monolithic glass. They discovered that some aspect ratios of layered glass experienced lower principal stresses than monolithic glass subjected to uniform, transverse loading in certain ranges of loading. Reznik and Minor [6] destructively tested different sizes of LG specimens at room temperature, 49 °C, and 170 °C. They compared the results with those from tests on monolithic glass lite specimens having the same dimensions. The testing led to very important conclusions; as temperature increases, LG behavior migrates towards the layered glass model. Norville [7] tested two lite specimens with aspect ratios of 1 and 2. His results were consistent with those of Reznik and Minor [6]. Behr et al. [8] studied LG beams at different temperatures. They found that traditional testing methods with the glass simply supported on two sides would not adequately account for the effect of aspect ratio on LG behavior. Vallabhan et al. [9] developed a mathematical model to analyze the LG plate. Experimental tests were conducted to validate the theoretical model. They found that the shear modulus varies as a function of the level of shear strain in the PVB interlayer at room temperature. Norville et al. [10] developed a theoretical, engineering mechanics model that accounts for the behavior of LG plates. Duser et al. [11] presented a model for stress analysis of laminated plates taking into account the PVB interlayer as viscoelastic material.

Recently, Asik and Tezcan [12] published a mathematical model of laminated glass beams, which is based on nonlinear strain–displacement relationship. The model was used to investigate the linear and nonlinear behavior of symmetric triplex glass beams in comparison with LG plate's behavior. Ivanov [13] presented a finite element model for LG beams. On his model, the distribution of strain and stress through the beam thickness and along its axis was obtained as a result of linear finite element analysis. He developed a mathematical model of triples glass beam, consisting of a bending curvature differential equation and a differential equation of PVB-interlayer shear interaction.

The objectives of the this paper can be summarized as following:

1. Studying the behavior of LG with PVB under a different range of temperatures. The effect of aspect ratio is considered.
2. Comparing the behavior of LG using PVB and HG/MD interlayer materials at room temperature.

A higher order finite element method (FEM) with nine nodes quadrilateral element was used in the analyses [14,15]. This FEM is designed for large deflections and rotation analysis of LG considering the effect of interlayer material under a different range of temperatures. The results obtained from the experimental study are compared with the corresponding FEM results and pronounced conclusions are obtained. El-Shami et al. [16] studied the structural behavior of glass plates other than rectangular shapes. They used a higher-order finite element model to analyze several examples with trapezoidal, rectangular, triangular, and hexagonal shaped glass plates (monolithic and LG).

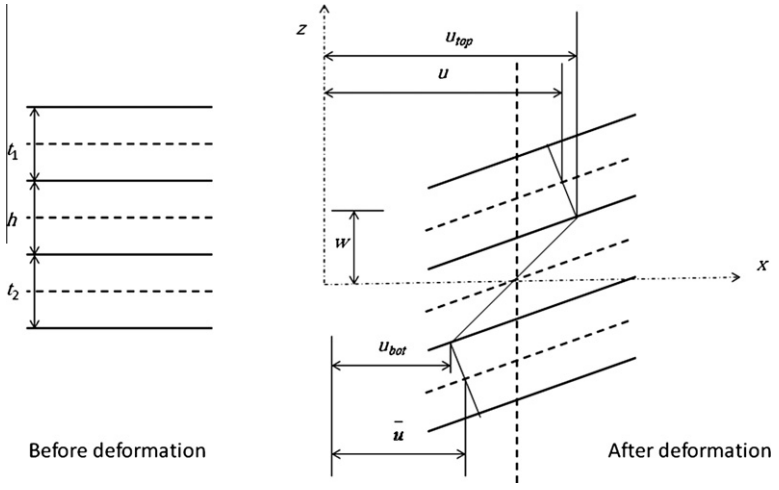

Figure 1 Undeformed and deformed geometries with respect to x and z axes.

2. Mathematical model

Since the theory of mindlin plate and solution techniques have previously been published in textbooks e.g., Cook et al. [17] and in papers e.g., Vallabhan et al. [9] and El-Shami et al. [16], only a brief account of the theory is presented here. The effect of interlayer material, on the laminated plate element is considered as shear strains γ_{xz} and γ_{yz} (Fig 1). The values of γ_{xz} and γ_{yz} can be calculated as:

$$\gamma_{xz} = \frac{u - \bar{u} + \theta_y\left(\frac{t_1+t_2}{2}\right)}{h} + w_{,x}$$

$$\gamma_{yz} = \frac{v - \bar{v} - \theta_x\left(\frac{t_1+t_2}{2}\right)}{h} + w_{,y}$$

where $u, \bar{u}, v$, and $\bar{v}$ are the displacements in the x and y directions, for the upper and lower plates; respectively, $w_{,x}$ and $w_{,y}$ are the first derivatives of deflection with respect to x and y; respectively and t_1, t_2, and h are the thicknesses of the upper and lower plates and the interlayer; respectively. The degrees of freedom will be increased by two for each node. Then the total number of degrees of freedom will be 63 per element; 7 d.o.f per node. To calculate the stiffness matrix, the relation between the displacements and the strains should be calculated. This relation is called [B] matrix [18]. This matrix can be calculated as;

$$\gamma_{xz} = [B_1]\{U\},$$
$$= \tfrac{1}{h}[N_i \quad 0 \quad -N_i \quad 0 \quad N_{i,x} \quad 0 \quad N_i\left(\tfrac{t_1+t_2}{2}\right) \quad \ldots] \quad \{U\}$$

where N_i denotes the shape function, and $\{U\}^T = \{u_i \quad v_i \quad \bar{u}_i \quad \bar{v}_i \quad w_i \quad \theta_{xi} \quad \theta_{yi} \ldots\}$ denotes the displacement vector for ith node in which $i = 1, 2, \ldots, 9$. Similarly,

$$\gamma_{yz} = [B_2]\{U\},$$
$$= \tfrac{1}{h}[0 \quad N_i \quad 0 \quad -N_i \quad N_{i,y} \quad N_i\left(\tfrac{t_1+t_2}{2}\right) \quad 0 \quad \ldots] \quad \{U\}$$

Then,

$$\{\gamma\} = \left\{\gamma_{xz} gamma_{yz}\right\} = [B]\{U\} = \begin{bmatrix} B_1 \\ B_2 \end{bmatrix}\{U\},$$

The stiffness matrix for the interlayer can be calculated as:

$$[K_{INT}] = \frac{1}{h}\iint [B]^T[D_G][B]dxdy = \frac{G_{INT}}{h}\iint [B]^T[I][B]dxdy$$

where $[K_{INT}]$ denotes the 63×63 interlayer stiffness matrix, G_{INT} denotes the modulus of rigidity for the interlayer, and $[I]$ denotes the identity matrix.

Because LG consists of two plates, this solution employs two different linear membrane stiffness matrices, two different nonlinear membrane stiffness matrices, and one linear bending stiffness matrix. The nonlinear stiffness matrix will be modified due to the fact that there are two plates. The total stiffness matrix for plates $[\overline{K}_P]$ can be written as:

$$[\overline{K}_P] = \begin{bmatrix} [K_{M1}]_{18\times18} & [0] & [K_{L1}]_{18\times27} \\ & [K_{M2}]_{18\times18} & [K_{L2}]_{18\times27} \\ Sym. & & [K_B + K_\sigma]_{27\times27} \end{bmatrix}$$

where $[K_{M1}]$ and $[K_{M2}]$ denote the linear membrane stiffness matrices for the upper and lower plate; respectively. $[K_{L1}]$ and $[K_{L2}]$ denote the nonlinear membrane stiffness matrices. $[K_B]$ denotes the linear bending stiffness matrix and $[K_\sigma]$ denotes the nonlinear stiffness matrix due to the membrane actions, i.e., the initial stress matrix [18].

$[\overline{K}_P]$ here is calculated in relation to $\{\underline{U}\}$, where $\{\underline{U}\}$ is given as;

$$\{\underline{U}\}^T = \{u_1 \quad v_1 \cdots u_9 \quad v_9 \quad \bar{u}_1 \quad \bar{v}_1 \cdots \bar{u}_9 \quad \bar{v}_9 \quad w_1 \quad \theta_{x1} \quad \theta_{y1} \cdots w_9 \quad \theta_{x9} \quad \theta_{y9}\}$$

Consequently, the authors must use a special transformation matrix $[T]$ to make the plate stiffness matrix $[\overline{K}_P]$ match with the displacement vector $\{U\}$, then

$$[K_P] = [T]'[\overline{K}_P][T]$$

The final stiffness matrix $[K]$ for LG takes the following form:

$$[K] = [K_p] + [K_{INT}]$$

3. Experimental procedure

Glass Research and Testing Laboratory (GRTL) staff tested different LG geometries, mainly two groups. Table 1 summarizes the geometries of group A specimens. The specimens have a PVB interlayer thickness of 0.762 mm. All the specimens were tested within a temperature range of 20–60 °C. The specimens of group B have a HG/MD interlayer thickness of 2.67 mm. Only one geometry was used as shown in Table 2. All specimens were tested under a temperature of 35 °C. Apecial type of strain gauge rosettes (CEA-060-062UR-350) was used. The strain gauges were temperature compensating and had an operating range of −75 to +175 °C. M-Bond AE 10 epoxy adhesive, with an operating range between −195 and 95 °C, bonded the gauges to the glass. The strain gauges were connected to the LG at the center and at the corner (50 mm from the edge). The test chamber, constructed of a 12.7 mm steel plate with four 203 mm steel channels welded onto it to form an open rectangular box, provided four sides support for the specimen. This test chamber provided support condition corresponding to ASTM E998 [19]. The steel chamber had four openings connected to the vacuum machine. As the vacuum was applied, the plate was loaded with negative pressure. The heating system consists of heating chamber, space heaters, heated blowers, and appropriate ductwork to distribute warm air over the surfaces of the test specimen. Four space

Table 1 Geometries of test specimens (group A).

Aspect ratio	Nominal specimen dimension (mm)	Design load (kPa)
1	1524 × 1524 × 12.7	4.57
2	965 × 1930 × 9.5	3.71
3	508 × 1524 × 6	4.39
4	508 × 2032 × 6	4.09
5	381 × 1905 × 6	6.49

Table 2 Geometries of test specimens (group B).

Aspect ratio	Nominal specimen dimension (mm)	Design load (kPa)
2	965 × 1930 × 7.85	3.71

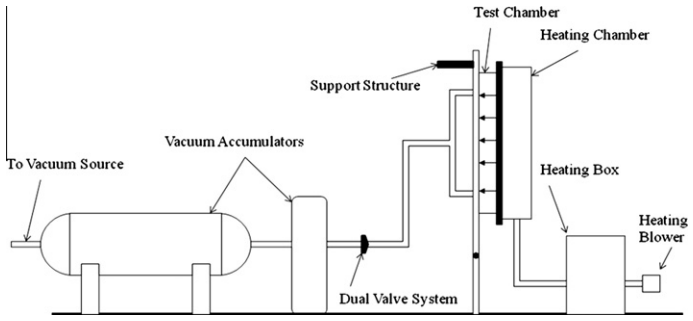

Figure 2 Experimental setup.

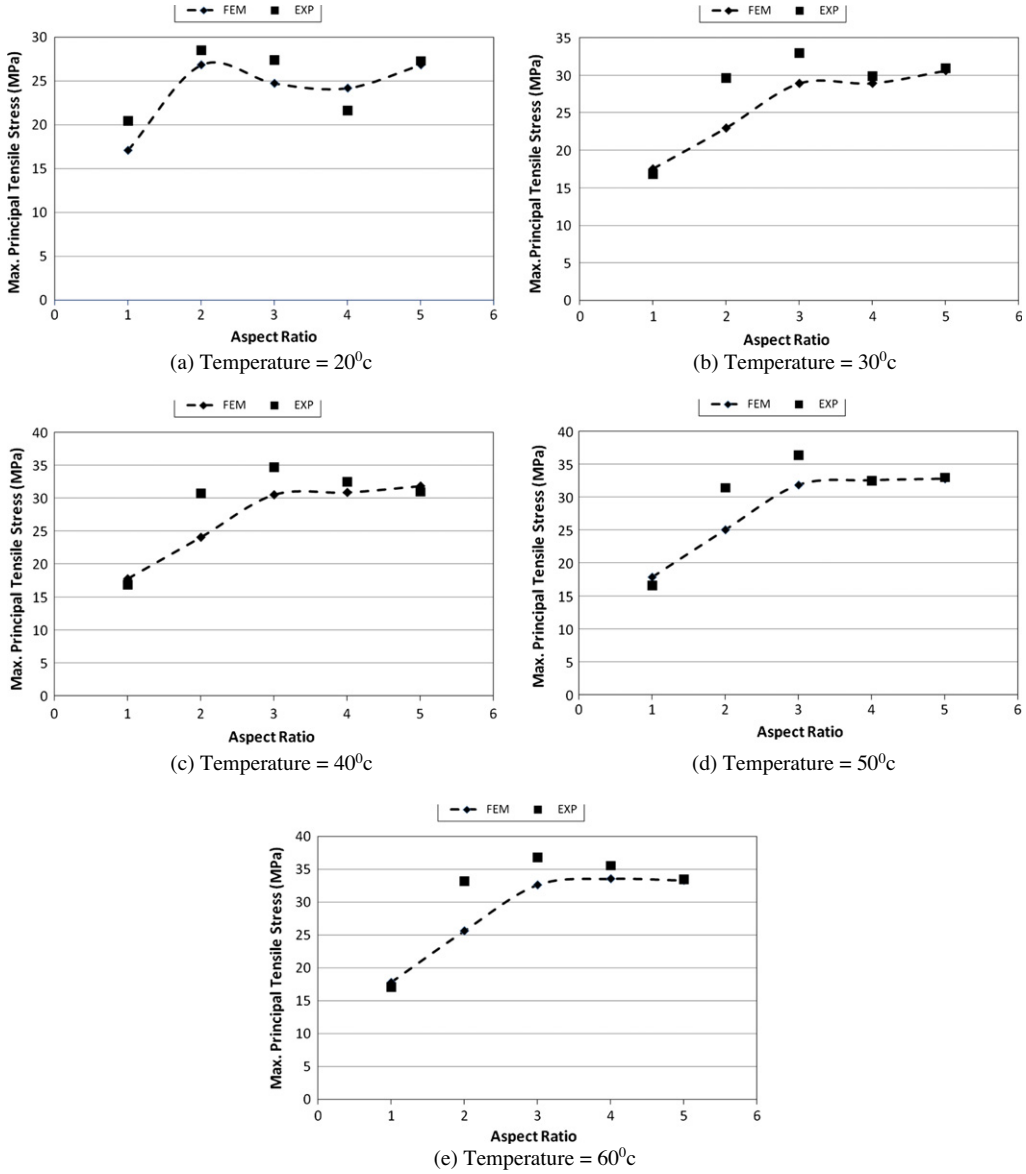

(a) Temperature = 20^0c

(b) Temperature = 30^0c

(c) Temperature = 40^0c

(d) Temperature = 50^0c

(e) Temperature = 60^0c

Figure 3 (a) Temperature = 20 °C. (b) Temperature = 30 °C. (c) Temperature = 40 °C. (d) Temperature = 50 °C. (e) Temperature = 60 °C.

heaters were used to warm the air inside the heating box. A heated blower was used to blow the pre-heated air (into the heated box) to the heating chamber. To start the proceeding, The GRTL staff removed the specimen from the crate. Then, they measured and record the thickness of the glass specimen at different locations and obtain an average thickness. The staff mounted the spacemen on the test frame. To control the temperature, GRTL staff mounted the heating chamber over the test chamber containing the glass specimen. They connected the heating box to the chamber and the heated blower to the box to start the heating processes. Two small holes with sliding covers, one located near to the center and another near the top of the heating chamber, allowed the staff to measure temperature. The hot air blown on the glass surface allowed the glass to reach the required temperature. Then, the researchers loaded the specimen to one-half the design load and the measurements were recorded. Finally they loaded the specimen to the design load and record the measurements. They repeated this procedure at different temperatures. Once the staff completed the test, they removed the specimen from the test chamber. Fig. 2 shows a sketch for the experimental setup.

4. Results of experiments versus theory

To verify the FEM, some problems have been solved and compared with the experimental results of previous researchers such as Vallabhan et al. [9]. The comparison showed very good agreement between the theoretical and the experimental results.

Fig. 3a–e shows the comparison between the FEM maximum principal stresses and the experimental results at the center of the plate at full design load for group A. The figures are for different aspect ratios, as given in Table 1, at different temperatures; 20, 30, 40, 50 and 60 °C; respectively. The corresponding values of shear modulus were 999.74, 317.16, 181.81, 91.01 and 44.82 kPa, respectively [20,21]. It should be noted that these values have been chosen for the corresponding temperatures. Direct shear testing can be used to determine the shear modulus for the interlayer material in LG. The figures show very good agreement between the FEM and experimental results. The average difference percentage between the results were 9.13%, 8.71%, 9.24%, 8.30% and 9.00% for the temperature cases of 20, 30, 40, 50 and 60 °C, respectively.

Fig. 4 shows the comparison between theoretical deflections at the center of the plates at different temperatures for aspect ratio 1 of group A. It can be seen from this figure that the deflection increases as the temperature increases. This is a direct result of the characteristic viscoelastic properties of PVB at high temperature [20]. This is clear in comparing with the curve of layered plates (see Fig. 4), in which the authors used modulus of rigidity equal to zero for PVB.

For group B, the comparison between the experimental and the theoretical deflections is shown in Fig. 5. It can be seen from Fig. 5 that there is a very good agreement between the theoretical and experimental results. The value of shear modulus for the HG/MD was chosen to be 1724 kPa [22]. Also, Fig. 5 shows the comparison between the LG with PVB interlayer and HG/MD interlayer; respectively. It is clears from Fig. 5 that the deflections for LG with PVB interlayer are higher than those of LG with HG/MD interlayer. Fig. 6 shows the maximum tensile principle stresses for group B for of LG plate

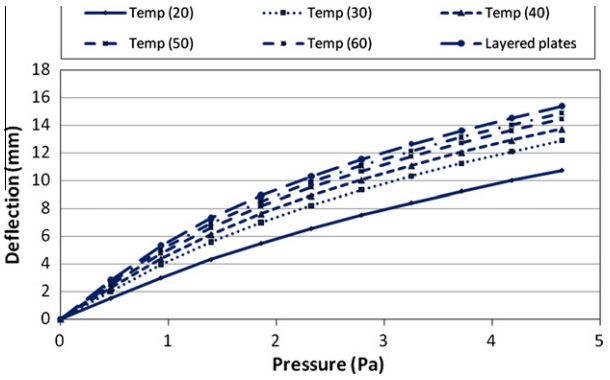

Figure 4 Deflection at the center of the plates at different temperatures for aspect ratio 1 of group A.

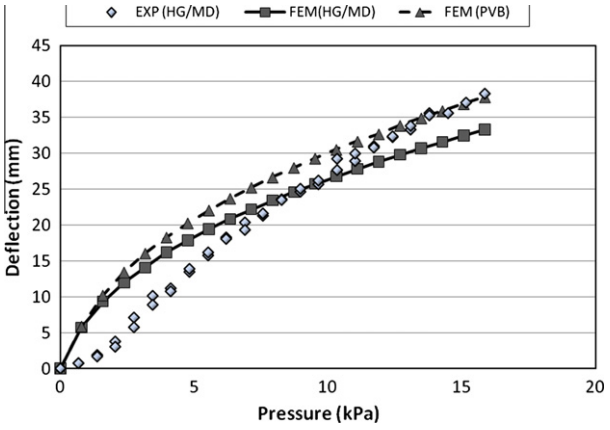

Figure 5 Deflections at the center of the plates for group B (aspect ratio = 2).

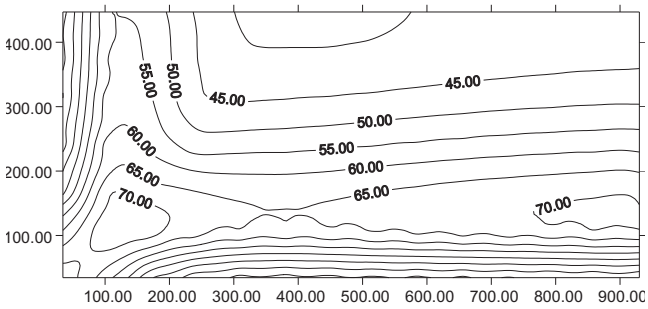

(a) LG with HG/MD interlayer

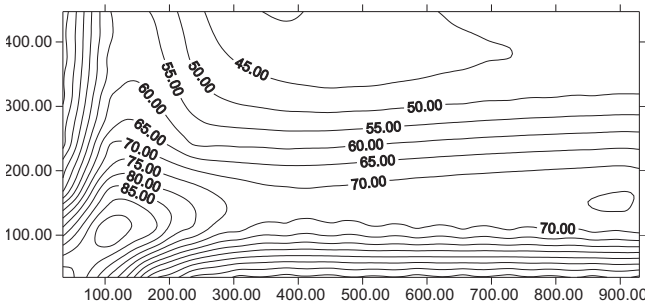

(b) LG with PVB interlayer

Figure 6 Maximum tensile stresses (MPa) for group B.

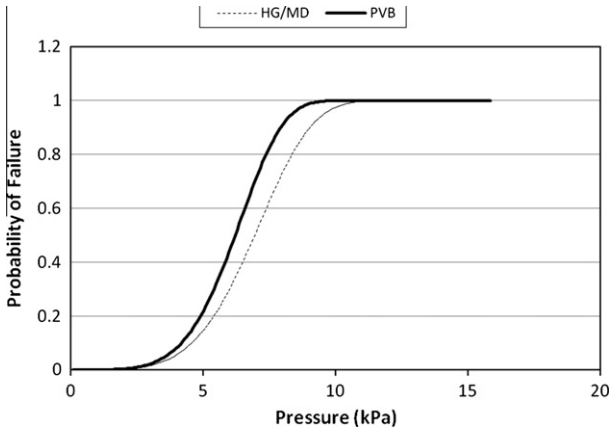

Figure 7 Probability of failure of LG with different interlayer type.

with PVB interlayer and HG/MD interlayer; respectively. It can be seen that using HG/MD interlayer decreases the maximum tensile principal stresses in comparison with PVB interlayer under the same load conditions.

Using the failure prediction methodology, the probability of breakage of a glass ply at the design load is [4];

$$P_B = 1 - \exp[-B]$$

where P_B is the probability which is used to be 0.008 [23] and B is the risk function, which can be calculated as;

$$B = k \int \int_{AREA} [c(x,y)\tilde{\sigma}_{\max}(x,y)]^m dxdy$$

where m and k denote the Weibull parameters [24], $c(x, y)$ denotes a stress correction factor at location (x, y), and $\tilde{\sigma}_{max}(x, y)$ is the maximum equivalent principal tensile stress at location (x, y). The authors noted that the probability of breakage of the LG with HG/MD interlayer is smaller than that of the LG with PVB interlayer (see Fig. 7). In other words, using HG/MD interlayer instead of PVB enhances the structural behavior of LG plates.

5. Conclusions

The objective of this paper was to investigate the structural behavior of LG with different interlayer materials. The factors used in the analysis were analytical results used FEM and experimental test results. The employed FEM takes into account the effect of the interlayer as a shear strain. Two types of experiments were considered for simply supported rectangular LG plates; one using PVB interlayer material with aspect ratios of 1, 2, 3, 4 and 5 under a range of temperature and the other using HG/MD interlayer at room temperature for aspect ratio 2. The agreement between the experimental and FEM results for both interlayer materials shows the capability of the present FEM to handle the effect of the different kinds of interlayer materials at different temperatures. The authors observe also that the effect of the interlayer material on transferred shear between the two glass plates is decreasing as the temperature is increasing for PVB interlayer. In general, LG with PVB interlayer comes close to the layered case at high temperature. Also the shear modulus of HG/MD is almost 2.5 times that of PVB. This will enhance the structural behavior of LG with HG/MD interlayer rather than that with PVB.

Acknowledgement

The experimental part of research described herein was conducted at the Glass Research and Testing Laboratory (GRTL) at Texas Tech. University.

References

[1] R. Quenett, The Mechanical Behavior of Laminated Safety Glass under Bending and Impact Stresses, Forgetragen auf dem DVM-Tag, Wurzburg (Germany), Manuskript-Eing., 1967.
[2] J.A. Hooper, On the bending of architectural laminated glass, International Journal of Mechanical Sciences (Great Britain) 15 (1973) 309–333.
[3] M.P. Linden, J.E. Minor, R.A. Behr, C.V.G. Vallabhan, Evaluation of Laterally Loaded Glass Units by Theory and Experiment, Glass Research and Testing Laboratory, Texas Tech University, Lubbock, Texas, 1983 (NTIS Accession No. PB84-216423).
[4] M.P. Linden, J.E. Minor, R.A. Behr, C.V.G. Vallabhan, Evaluation of Laterally Loaded Glass Unites by Theory and Experiment, Supplemental Report No. 1. Glass Research and Testing Laboratory, Texas Tech University, Lubbock, Texas, 1984 (NTIS Accession No. PB85-111532).
[5] S.R. Nagalla, C.V.G. Vallabhan, J.E. Minor, H.S. Norville, Stresses in Layered Units and Monolithic Glass Plates, Glass Research and Testing Laboratory, Texas Tech University, Lubbock, Texas, 1985 (NTIS Accession No. PB86-142015/AS).
[6] P.L. Reznik, J.E. Minor, Failure Strengths of Laminated Glass Units, Glass Research and Testing Laboratory, Texas Tech University, Lubbock, Texas, 1986 (NTIS Accession No. PB87-118873/AS).
[7] H.S. Norville, Breakage Tests of Du Pont Laminated Glass Units, Glass Research and Testing Laboratory, Texas Tech University, Lubbock, Texas, 1990.
[8] R.A. Behr, J.E. Minor, H.S. Norville, Structural behavior of architectural laminated glass, Journal of Structural Engineering, ASCE 119 (1993) 202–222.
[9] C.V.G. Vallabhan, Y.C. Das, M. Magdi, M. Asik, J.R. Bailey, Analysis of laminated glass units, Journal of Structural Engineering, ASCE 119 (5) (1993) 1572–1585.
[10] H.S. Norville, K.W. King, J.L. Swofford, Behavior and strength of laminated glass, Journal of Engineering Mechanics, ASCE 124 (1) (1998) 46–53.
[11] A.V. Duser, A. Jagota, S.J. Bennison, Analysis of glass/polyvinyl butyral laminates subjected to uniform pressure, Journal of Engineering Mechanics, ASCE 125 (4) (1994) 435–441.
[12] M.Z. Asik, S. Tezcan, A mathematical model for the behavior of laminated glass beams, Computers and Structures 83 (2005) 1742–1753.
[13] I.V. Ivanov, Analysis, modeling, and optimization of laminated glasses as plane beam, International Journal of Solids and Structures 43 (2006) 6887–6907.
[14] M.M. El-Shami, C.V.G. Vallabhan, S.A. Kandil, Comparison of nonlinear Von Karman and Mindlin plate solutions, in: Proceedings of the Texas ASCE Conf., Spring Meeting, Houston, Texas, 1997.
[15] M.M. El-Shami, H.S. Norville, Finite element modeling of architectural laminated glass, IES Journal Part A: Civil and Structural Engineering, Taylor & Francis 4 (1) (2011) 8–16.

[16] M.M. El-Shami, Y.E. Ibrahim, M. Shuaib, Structural behavior of architectural glass plates, Alexandria Engineering Journal 49 (2010) 339–348.
[17] R.D. Cook, D.S. Malkus, M.E. Plesha, Concepts and Applications of Finite Elements Analysis, John Wiley & Sons, Inc., 1989.
[18] O.C. Zienkiewicz, The Finite Element Method, McGraw-Hill Book Co., New York, 1977.
[19] ASTM, Standard Test Method for Structural Performance of Glass in Windows, Curtain Walls, and Doors under the Influence of Uniform Static Loads by Nondestructive Methods, E998-84, West Conshohocken, PA, US, 2006.
[20] G. Krüger, Temperature effects on the structural behavior of laminated safety glass, Otto-Graf Journal 9 (1998) 153–163.
[21] S.J. Bennison, M.H.X. Qin, P.S. Davies, High-performance laminated glass for structurally efficient glazing, in: Proceedings of Innovative Light-weight Structures and Sustainable Facades, Hong Kong, 2008.
[22] T. Mackay, H.S. Norville, Strain Measurements in Laminated Glass, Glass Research and Testing Laboratory, Texas Tech University, Lubbock, TX, 2001.
[23] ASTM, Standard Test Method for Structural Performance of Glass in Windows, Curtain Walls, and Doors under the Influence of Uniform Static Loads by Nondestructive Methods, E998-84, West Conshohocken, PA, US, 2009.
[24] W.L. Beason, J.R. Morgan, Glass failure prediction model, Journal of Structural Engineering, ASCE 110 (2) (1984) 197–212.